AD-A052 881 SOUTHWEST RESEARCH INST SAN ANTONIO TEX DEPT OF MAT--ETC F/G 20/11
CHARACTERIZATION OF FATIGUE CRACK TIP DEFORMATION.(U)
FEB 78 J LANKFORD, D L DAVIDSON F44620-75-C-0050

UNCLASSIFIED AFOSR-TR-78-0490 NL

| OF |
AD
A052881

END
DATE
FILMED
5-78
DDC

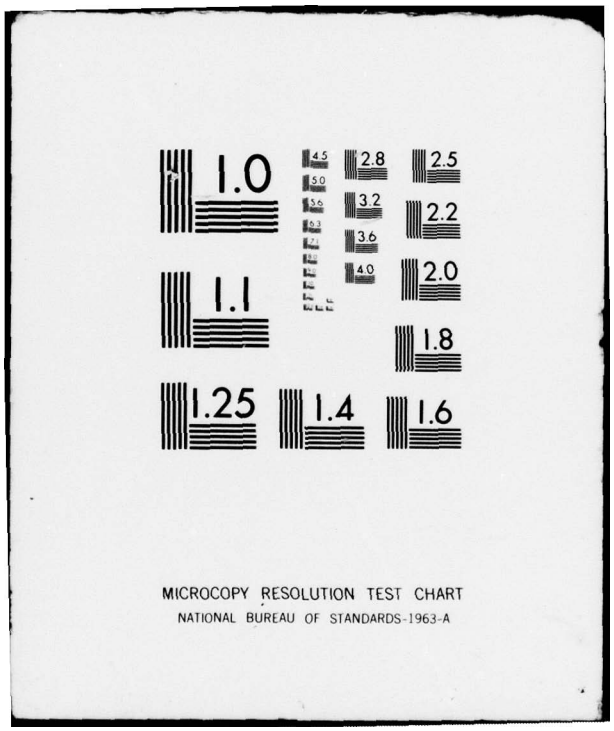
1.0
1.1
1.25
1.4
1.6
1.8
2.0
2.2
2.5
2.8
3.2
3.6
4.0
4.5
5.0
5.6
6.3
7.1
MICROCOPY RESOLUTION TEST CHART
NATIONAL BUREAU OF STANDARDS-1963-A

Characterization of Fatigue Crack Tip Deformation

AFOSR Final Scientific Report

February 1978

By
James Lankford
David L. Davidson

Southwest Research Institute
San Antonio, Texas 78284

AFOSR Contract F44620-76-C-0050
Work Unit No. 2307/A7

Characterization of Fatigue Crack Tip Deformation

AFOSR Final Scientific Report

February 1978

by
James Lankford
David L. Davidson

Southwest Research Institute
San Antonio, Texas 78284

This research was sponsored by the Air Force Office of Scientific Research, Directorate of Electronics and Solid State Sciences, under Contract F44620-75-C-0050.

Approved for release; distribution unlimited.

APPROVED:

U. S. Lindholm, Director
Department of Materials Sciences

REPORT DOCUMENTATION PAGE — BEFORE COMPLETING FORM

1. REPORT NUMBER: AFOSR-TR-78-0490	2. GOVT ACCESSION NO.
3. RECIPIENT'S CATALOG NUMBER	
4. TITLE (and Subtitle): Characterization of Fatigue Crack Tip Deformation	5. TYPE OF REPORT & PERIOD COVERED: Final Report 1 Jan 75 — 31 Dec 77
	6. PERFORMING ORG. REPORT NUMBER
7. AUTHOR(s): James Lankford, Jr. and David L. Davidson	8. CONTRACT OR GRANT NUMBER(s): F44620-75-C-0050
9. PERFORMING ORGANIZATION NAME AND ADDRESS: Southwest Research Institute, Department of Materials Sciences, San Antonio, Texas 78284	10. PROGRAM ELEMENT, PROJECT, TASK AREA & WORK UNIT NUMBERS: 61102F; 2306/A1
11. CONTROLLING OFFICE NAME AND ADDRESS: AF Office of Scientific Research, Bolling AFB, Building 410, Washington, D.C. 20332	12. REPORT DATE: February 1978
	13. NUMBER OF PAGES: 14
14. MONITORING AGENCY NAME & ADDRESS (if different from Controlling Office)	15. SECURITY CLASS. (of this report): Unclassified
	15a. DECLASSIFICATION/DOWNGRADING SCHEDULE

16. DISTRIBUTION STATEMENT (of this Report)

Approved for public release; distribution unlimited.

17. DISTRIBUTION STATEMENT (of the abstract entered in Block 20, if different from Report)

18. SUPPLEMENTARY NOTES

19. KEY WORDS (Continue on reverse side if necessary and identify by block number)

Fatigue, crack growth, aluminum alloys, electron channeling, crack tip plasticity, overloads, retardation

20. ABSTRACT (Continue on reverse side if necessary and identify by block number)

During the past three years, fatigue crack tip plasticity and overload-induced fatigue crack retardation have been studied using several complementary techniques, especially selected area electron channeling and high resolution SEM observation of crack tips under various stages of loading. It is found that while some materials exhibit plastic yielding behavior in agreement with existing theory, some materials, especially aluminum alloys, diverge widely both from one another and from theory. In particular, for equivalent stress intensities, overload ratios, and pre-overload crack growth rates, the

Concl page

DD FORM 1 JAN 73 1473 EDITION OF 1 NOV 65 IS OBSOLETE

Unclassified

SECURITY CLASSIFICATION OF THIS PAGE (When Data Entered)

20.

retardation period (in cycles) for 2024-T3 significantly exceeds that for 6061-T6 and 7075-T6. This behavior is intimately related to the size and shape of the overload plastic zone, variations in which probably are controlled by the plastic flow rules for the alloys. Based on the channeling results, a qualitative model has been developed to explain the several "stages" of retardation. In addition, plastic zone calculations and measurements made by a variety of techniques have been correlated, and general guidelines have been suggested for estimating plastic zone parameters, and evaluating the physical significance of the results of various measurement approaches. Results indicate that the generally accepted calculations for crack tip parameters are often misinterpreted, and that yield stress alone may be insufficient as a normalizing factor in calculating plastic zone size. Study also has shown that by appropriate SEM procedures, dislocation subcells lying within the inner, "reverse cyclic" plastic zone may be imaged in bulk specimens of certain materials. This procedure looks promising as a way of understanding certain load spectrum, alloying, and environmental effects.

TABLE OF CONTENTS

LIST OF ILLUSTRATIONS

I. Introduction

Understanding the response of metals to stress cycling is important so that (1) the lifetimes of engineering structures can be predicted, and (2) better structural materials can be developed. Since many structures contain cracks inherent to their fabrication, the study of fatigue crack propagation has become an important part of our understanding of the response of such structures to cyclic loading

Fatigue crack propagation (FCP) occurs because of certain events which take place within the plastically strained region (plastic zone) attending the crack tip. Understanding and prediction of phenomena such as overload retarded crack growth, load spectra interactions, and the effect of alloying and other metallurgical factors on these aspects of FCP depends upon knowledge of such parameters as plastic zone size and shape, the strain distribution within this zone, crack tip opening displacement, and the crack opening mechanism. This report summarizes the results of a three year study of fatigue crack tip plasticity, emphasizing aerospace aluminum alloys, but including others where appropriate. Several novel approaches to crack tip study have been developed, including selected area electron channeling, crack tip replication, and recently, servo-controlled, closed-loop cycling of specimens under observation within the SEM.

This report will present the objectives toward which the study was focused, and summarize the most essential achievements. Experimental details and complete discussions of results are contained in the attached technical publication list.

II. Research Goals

The general goal of this program is to study fatigue crack growth in aerospace materials through determination of crack tip plasticity parameters which determine the response of the material to the loading imposed. The specific objectives of the program were as follows:

- Determine the effect of aluminum alloy composition upon plastic zone parameters during monotonic stress cycling.
- Determine the effect of aluminum alloy composition upon overload plastic zone/fatigue crack growth interaction.
- Evaluate plastic zone size dependencies in different materials.
- Evaluate sensitivities of various plastic zone size measuring techniques.
- Determine the relationship between surface and interior plastic zones.
- Determine role of crack tip subcells in fatigue of various materials.

- Evaluate certain factors (tensile versus compressive plastic strain, image rotation) which may cause special problems in applying the electron channeling approach to fatigue studies.

- Establish crack tip deformation and incremental crack growth mechanisms.

III. Summary of Research

1. Monotonic Fatigue Plastic Zone Size

Electron channeling measurements carried out on several alloys have been analyzed and compared with other measurement techniques and with various theoretical calculations. Alloys studied by electron channeling included 6061-T6, 2024-T4, and 7075-T6 aluminum, low carbon steel, 304 stainless steel, and Fe-3Si steel; other materials which were studied by investigators using different approaches (interferometry, etch-pitting, x-ray diffraction) included single and polycrystalline copper, other stainless steels, maraging steels, INCO 718, and Al-1/2 Mg. It was found that there exists only limited agreement between theory and experimental measurements, but that conclusions concerning the appropriate plastic zone dimensions for certain alloys and crack tip conditions could be drawn.

For example, for most of the materials, with the notable exception of Al alloys, a good estimate of the maximum monotonic plastic zone dimension r_p can be obtained using

$$r_p = \alpha\left(\frac{K}{\sigma_y}\right)^2$$

with α a material independent constant, K the maximum stress intensity, and σ_y the tensile yield stress. The value of K ranged from 9-12 MN $m^{-3/2}$, with a cyclic stress ratio of 0.05. As expected, the results can be rationalized womewhat on the basis of plane stress-plane strain considerations, with measurements taken on specimen surfaces tending to reflect a predominantly plane stress (Pσ) situation, and midplane or interior measurements being more nearly plane strain (Pε). Averaging all of the α's generated from surface measurements yields $\alpha_{P\sigma} \approx 0.1$, with the lowest corresponding theoretical estimate being ~0.16. Similarly, the average of the interior measurements gave $\alpha_{P\varepsilon} \approx 0.06$, again below the lowest theoretical calculation, ~.14.

For most of the materials studied, it was possible to determine zone r_p^c, which was predicted with remarkable consistency by

$$r_p^c = \alpha'\left(\frac{\Delta K}{\sigma_y}\right)^2$$

where $\alpha' \approx 0.01$, independent of the state of stress, and ΔK is the cyclic stress intensity.

The electron channeling results for plastic zone shape and size agree quite well with dislocation etch-pit results of Hahn and co-workers for silicon steel. However, similar measurements carried out using stainless steel indicated significantly larger plastic zones than provided by microhardness studies. The cause of this discrepancy was investigated by performing microhardness tests and electron channeling measurements on calibrated 316 stainless steel tapered tensile specimens. An increase in hardness was indiscernible until a strain of ~6% was attained, in contrast to the electron channeling results, which showed the least detectable plastic strain to be ~0.4%. Consequently, it appears that the difference can be resolved simply on the basis of greater sensitivity on the part of electron channeling to small plastic strain amplitudes.

This sensitivity was important in discriminating differences in the plastic zone boundaries for the three commercial aluminum alloys studied. Figure 1 shows, for example, the degradation in electron channeling pattern quality caused by barely crossing over into the plastic zone of a fatigue crack tip in 7075-T6. Note in particular the destruction (Figure 1(b)) within the zone of the fine structure and higher order reflections present in the equivalent pattern obtained at a point just outside the boundary (Figure 1(a)). Comparison of the maximum plastic zone dimensions of the three alloys gave surprising results, i.e., for 6061-T6, $\alpha = 0.13$; for 2024-T4, $\alpha = 0.5$; for 7075-T6, $\alpha = 0.79$. According to theory, all of the α's should be identical, and approximately equal to some plane stress value, since the measurements were made at the surface of the specimen. It is clear, however, that in this case α is <u>not</u> material independent. In fact, the largest α pertains to 7075-T6, which because of its strength would be expected to be most consistent with plane strain, hence a small α. Vice versa was true for 6061-T6 and 7075-T6, the monotic strain hardening coefficient = 0.03, and the cyclic coefficient = 0.05. In addition, theoretical studies indicate that even quite large strain hardening differences would alter the plastic zone size only slightly.

For the stress intensity range studied, all of the specimens were sufficiently thick ($t - 2.5$ mm $> t_{min}$) that conditions of plane strain should have prevailed all along the crack tip except at the specimen surface, so that one might expect the channeling results to yield an α somewhere between the theoretical values for plane strain and plane stress. This was not the case, with α for 6061-T6 being below the minimum theoretical plane strain prediction, and for 7075-T6 being in excess of the maximum theoretical plane stress values. A 6061-T6 specimen was sectioned to look for thru-thickness variation in plastic zone size, but none was found. Fracture surface examination also revealed no difference in topography through the specimen thickness. One is led to the tentative conclusion that α depends upon some material property other than yield strength.

For 2024-T4, the results of plastic zone size determination by electron channeling, interferometry, and plane stress theory are all in reasonable agreement. Disagreement between the electron channeling and interferometry results on 7075-T6, whereby the electron channeling determination of α exceeds that obtained through interferometry by some 60%, are presently unexplained. Taken by themselves, these data would imply a

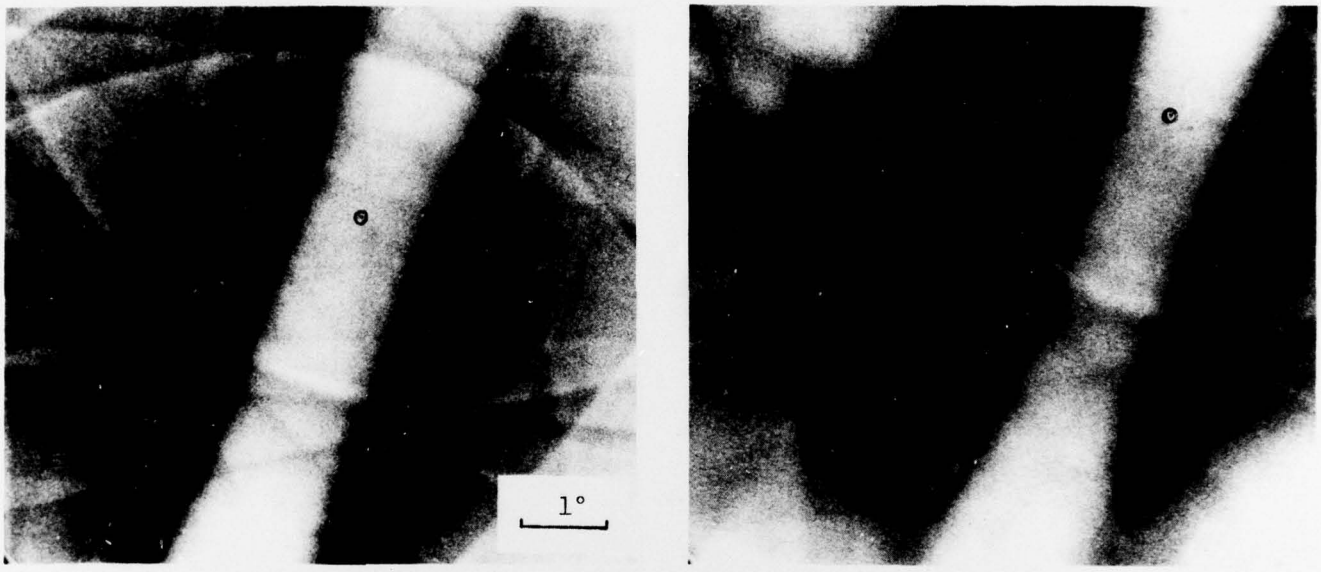

Outside (a)

Inside (b)

Figure 1. Channeling patterns from either side of the plastic zone boundary in 7075-T6 showing the relative change in line acuity associated with traversing the boundary. The small circle denotes the < 123 > zone axis. Angular coverage by the patterns is shown.

higher sensitivity to plastic strain on the part of the electron channeling technique.

At least two factors suggest themselves as possible explanations for the observed plastic zone relationships: (1) environmental influences, and (2) differences in crack tip yielding mechanisms. In order to examine these possibilities, we are currently carrying out additional tests in an inert environment (since this is a basic assumption of most theories), and examining crack tip yielding processes in all three alloys, using a special load-cycling stage mounted within the SEM chamber.

2. Overload Plastic Zone/Fatigue Crack Tip Interaction

One of the major goals of this program has been to utilize the techniques of selected area electron channeling and high resolution SEM to understand the relationship between overload-induced crack growth retardation and the overload plastic zone. Our early work employed 6061-T6 aluminum, but during the last two years, we were able to extend the effort to include 2024-T4 and 7075-T6.

Most of our experiments have been carried out in zero-tension cycling at pre-overload stress intensities of 10-12 MN $m^{-3/2}$, at a frequency of 10 Hz, and under ambient conditions. Overload ratios of 50%, 100% and 150% have been used to cause spike overload crack retardation. Following each overload, the plastic zone has been determined using electron channeling, and the subsequent growth of the crack has been documented with respect to the zone. A number of important facts have emerged from recent studies.

Following an overload, the previously discussed relationships for maximum plastic zone dimensions hold fairly well. However, it turns out that this parameter does not relate to the actual overload retarded crack length; rather, the controlling plastic zone dimension is the distance at the time of the overload from the crack tip to the nearest point on the overload plastic zone boundary. This point, for all three alloys, tends to be located between the two "arms" of the overload zone which arcs out and around in front of the crack. At an overload of around 200%, the arms apparently come together, at which point the minimum and maximum plastic zone dimensions essentially coincide.

If one assigns an α_{min} as the coefficient in the previous expression for plastic zone size which corresponds to the minimum distance separating the crack tip and overload boundary, an interesting picture emerges. In terms of this parameter, the alloys would be ordered as follows: 6061-T6, 7075-T6, 2024-T4, with 2024-T4 having the largest α_{min}. This is also the order in which the alloys rank with regard to the average number of delay cycles for a given overload, with 2024-T4 exhibiting the largest delay. (This agrees with interferometry work by Chanani on 2024-T4 and 7075.) In this case, the difference may well relate to strain hardening, since 2024-T4 has a significantly larger monotonic strain hardening coefficient than 6061-T6 and 7075-T6, which have equal coefficients and similar retardation behavior. For 6061-T6, most of the overload zone is located out to the sides of the crack, while for 2024-T4 more of the zone is "com-

pressed" ahead of the crack, creating a blunter zone configuration.

For each material, the post-overload crack follows (at a very reduced growth rate) a path which corresponds to the direction to the nearest segment of the elastic-plastic boundary, at which point the growth rate increases dramatically (Figures 2, 3). If the separation of the overload arms is greater than the width of the pre-overload, steady-state plastic zone, the rate returns to the pre-overload rate. If not, the rate remains slightly lower than the pre-overload rate until the crack passes beyond the point at which its steady-state plastic zone no longer touches the overload zone.

There are several implications from these results. First, alloying does make a difference in crack retardation, by altering the overload plastic zone size and shape. The relationship for predicting plastic zone size appears to be alloy specific through some parameter in addition to yield strength (possibly the plastic flow characteristics). Finally, the retardation period occurs over a plastic zone dimension which for overloads of 100% or less is much smaller than the maximum plastic zone size. This dimension is the distance from the crack tip at the [illegible]e of the overload to the nearest point on the elastic-plastic boundary, and the distance is alloy sensitive, even when yield strengths are nominally identical.

3. Fatigue Crack Tip Subcell Structures

Many crack growth models include an explicit dependence upon a microstructural "element" characteristic of the crack tip, usually assumed to be dislocation cell size. If so, this element size and its spacial extent should also be dependent upon ΔK. Therefore, an electron channeling contrast study of this parameter was undertaken using low carbon steel as a material, since cells form more readily in this material than in 6061-T6 aluminum, and in addition are generally larger. The material was provided us by T. Yokobori, in the form of fatigue specimens already studied using the X-ray microbeam (XMB) technique. A number of interesting facts were noted. First, subgrain size decreased as the crack tip was approached, the minimum size being approximately one micron, regardless of stress intensity. This affords an interesting correlation with the study of ε_p versus ΔK in 6061, where a saturation value for ε_p near the crack tip also was noted. Moreover, the distance from the tip at which subgrains are formed increased with ΔK, again in agreement with the increase in cyclic zone boundary found in the 6061 work. The channeling contrast results agreed excellently with earlier XMB observations, and plastic zone size claculations based on subgrain formation agreed reasonably well with theoretical predictions (Figure 4).

Additional experiments have been carried out using the three aluminum alloys. While subcells in 6061-T6 and 2024-T4 were found to be difficult, if not impossible to resolve, we did have some success with 7075-T6. An example of the subcells attending a crack tip is shown in Figure 5, in which subcells, plastic surface deformation, and classic crack blunting via crack tip slip-off can be seen. Further work is required to quantify subcell distributions in aluminum alloys.

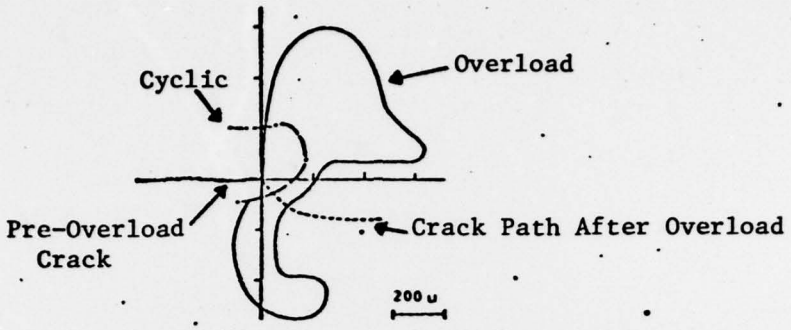

(a) --Cyclic and overload plastic zone boundaries and their relation to post-overload crack growth, 6061-T6 alloy, 100% overload, ΔK = 10.5 $MN/m^{3/2}$

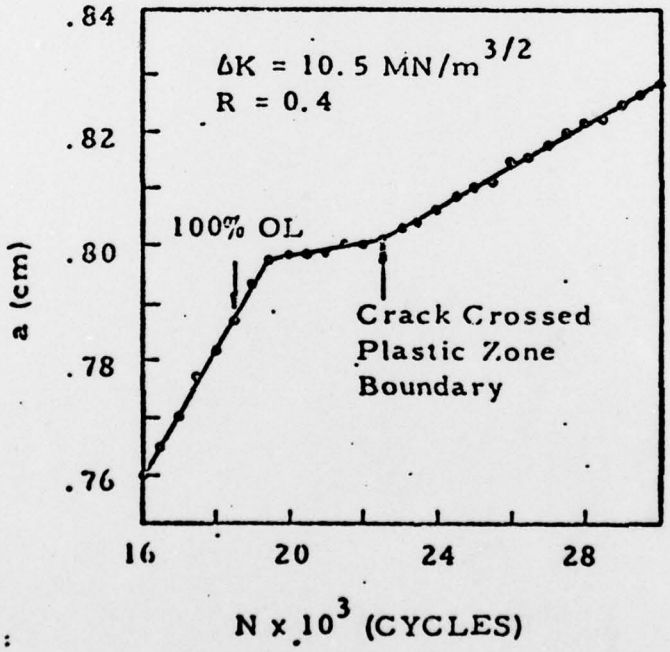

(b) --Crack growth versus cycles for overload test shown in (a)

FIG. 2 --Typical Overload Zone/Post-Overload Crack Growth Relationship

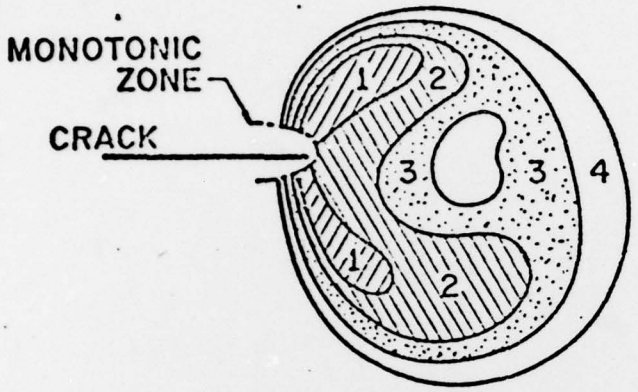

1. 50% OVERLOAD ZONE
2. 100% OVERLOAD ZONE
3. 150% OVERLOAD ZONE
4. 200% OVERLOAD ZONE

a) Overload zone development

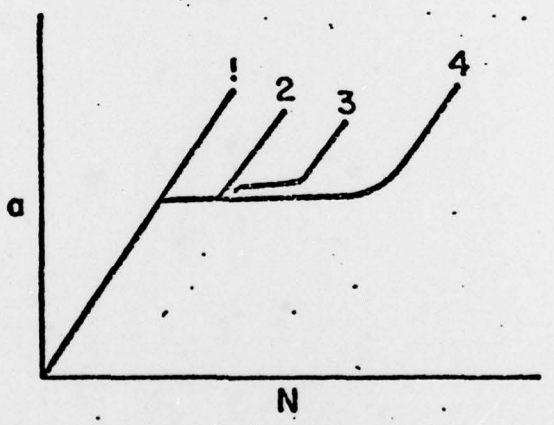

b) Crack length (a) versus cycles (N) for overload zones sketched in a)..

FIG. 3 -- Schematic Illustration of Overload Zone Shape Upon Post-Overload Fatigue Crack Growth

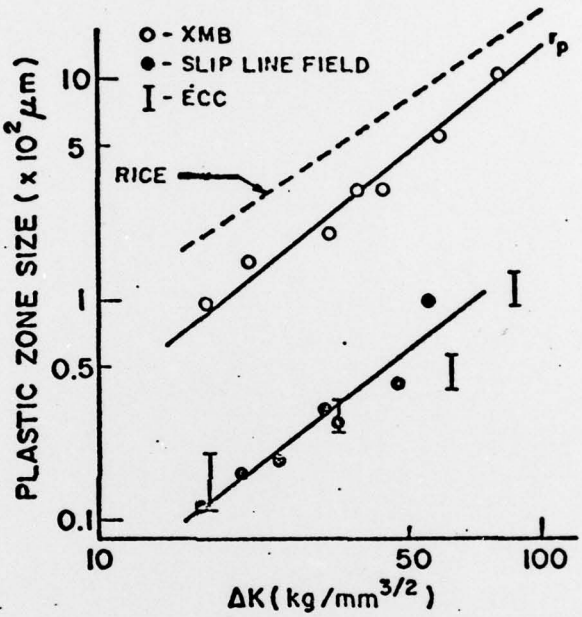

FIG. 4. --Monotonic and Cyclic Plastic Zone Size in Low Carbon Steel

Figure 5. Subcell formation in the vicinity of a fatigue crack tip subjected to a one cycle overload of $K = 26MN/m^{3/2}$ as observed by channeling contrast. 7075-T6 Aluminum Alloy, 20 keV

4. Relation of Compressive Versus Tensile Cycling to Electron Channeling Pattern Characters

Experiments were run to determine whether equivalent cyclic strains accumulated under compressive versus tensile loading showed differences in their channeling patterns. No differences were observed, indicating the validity and general applicability of our technique for correlating channeling pattern quality with strain using a specimen deformed varying amounts in tension.

5. Image Rotation in Electron Channeling

The electro-magnetic and geometric conditions characteristic of specimen image-channeling pattern rotation in our SEM were determined, and compared with the corresponding relationship for other systems for producing patterns. This work was necessary in order for us to accurately interpret crystallographic orientation effects in deformed or fatigued specimens.

6. Crack Tip Deformation in 304 Stainless Steel - A Model

At low and intermediate values of ΔK, crack growth rates in austenitic stainless steels are significantly smaller than corresponding striation spacings, until higher stress intensities, where they agree. It generally is assumed that incremental crack front advance is responsible for this behavior. Our work indicates that for 304 stainless, this is not the case; rather, crack advance probably is continuous across the specimen thickness. SEM observation of sequentially loaded crack tips shows that cyclic strain hardening of crack tip slip bands forces crack growth rates to lag striation spacings, in that crack advance does not take place until band hardening is complete and a new band activated in previously lightly or undeformed material adjacent to the old band ahead of the crack tip. At low stress intensities, many cycles are required to harden a band, hence a large discrepancy between growth rate and striation spacing, while at high ΔK values, bands harden very quickly, and cyclic crack advance is almost equal to a shear band per cycle.

IV. Conclusions and Implications

A number of general conclusions may be drawn from the preceding discussion; these have implications in terms of technological applications.

1. Plastic zone sizes in aluminum alloys exhibit a dependence upon factors other than yield strength, contrary to current theory; these factors may relate to strain hardening, crack tip yielding mechanism, or environment. The usual assumption of a simple yield strength relationship thus leads to significant error in calculations involving plastic zone size. For many other materials, the measured value for plastic zone size turns out

to be smaller than that predicted by theory, but nevertheless dependent principally on yield strength. The aluminum alloy results in particular have considerable application, since many problems of current relevance, such as stress corrosion, corrosion fatigue, and hydrogen embrittlement, involve calculation of the dimensions of the defect-rich crack tip plastic zone. The results also shed light on the relationship between state of stress and the degree of crack tip plasticity in engineering materials.

2. Crack retardation depends sensitively upon overload plastic zone size and shape. The excellent correlation between the overload-affected crack length and the minimum plastic zone dimension implies that crack tip plasticity, and not crack closure in the wake of the crack, is the pre-eminent factor in overload retardation. Moreover, the results show how models for overload-induced retardation, such as those of Willenburg and Wheeler, may be modified to more accurately reflect the shape and size of the overload zone. This would in principal allow prediction of the most efficient overload sequencing into order to maintain a minimum retarded growth rate. However, the present results regarding the overload-affected crack length must be complemented by further study of the period of retardation. This must be related to the degree of residual stress present in the overload zone, hence to the strain hardening (energy-absorbing) characteristics of the material. Therefore, we are trying to quantify our currently qualitative retardation model by extending it to include the strain distribution within the overload zone, and from this estimate the lowered effective stress intensity responsible for the reduced rate of growth experienced by a crack passing through the zone. This extension involves mapping of the strain distribution within overload zones using electron channeling pattern analysis of calibrated tensile specimens. If successful, this work will help tie together previously unrelated studies by various investigators, permit ranking of materials in terms of their likely resistance to crack growth under spike overload conditions, and ultimately, allow the prediction of retarded growth rates within overload zones in aerospace alloys.

3. Crack tip subcell structures in some iron and aluminum based alloys can be imaged through certain contrast effects when the SEM is operated in the backscattered mode. This provides a unique opportunity to study crack-subcell relationships in bulk specimens, rather than resort to thin foil, TEM techniques, or etching of special, non-aerospace materials like Fe-3Si, as has been required heretofore. The results obtained are thus relevant to the scale of size of actual engineering structures, an important consideration when trying to extend laboratory results to the prediction of lifetimes under service conditions.

PUBLICATIONS (AFOSR Sponsorship)

1. D. L. Davidson, "A Method for Quantifying Electron Channeling Pattern Degradation Due to Material Deformation," Proceedings, Seventh Annual Scanning Electron Microscope Symposium, IIT Research Institute, pp. 927-934, 1974.

2. D. L. Davidson, "Electron Channeling: A New Metallurgical Tool," Research/Development, 25, 9, pp. 34-40, September 1974.

3. J. Lankford and J. G. Barbee, "SEM Characterization of Fatigue Crack Tip Deformation in Stainless Steel Using a Positive Replica Technique," Journal of Materials Science, 9, pp. 1906-1908, 1974.

4. D. L. Davidson, "Fatigue Crack Plastic Zone Size and Shape Through the Specimen Thickness," International Journal of Fracture, 11, pp. 1047-1048, 1975.

5. J. Lankford and D. L. Davidson, "Fatigue Crack Tip Plasticity Associated with Overloads and Subsequent Cycling," ASME Journal of Engineering Materials and Technology, 98(1), Series H, pp. 17-23, 1976.

6. D. L. Davidson and J. Lankford, "Plastic Strain Distribution at the Tips of Propagating Fatigue Cracks," ASME Journal of Engineering Materials and Technology, 98(1), Series H, pp. 24-29, 1976.

7. D. L. Davidson, "Rotation Between SEM Micrograph and Electron Channeling Patterns," Journal of Physics E (Scientific Instruments), 9, p. 341, 1976.

8. D. L. Davidson, J. Lankford, T. Yokobori, and K. Sato, "Fatigue Crack Tip Plastic Zones in Low Carbon Steel," Engineering Fracture Mechanics, 12(4), p. 579, 1976.

9. J. Lankford and D. L. Davidson, "Discussion of Plastic Zone Sizes in Fatigued Specimens of Inco 718," Metallurgical Transactions, A, 7A, p. 1044, 1976.

10. D. L. Davidson, "Applications of Electron Channeling to Materials Science," Proceedings, Electron Microscopy of America Annual Meeting, p. 402, 1976.

11. D. L. Davidson, "Nondestructive, Near-Surface Plasticity Determinations by Electron Channeling," Surface Effects in Crystal Plasticity, ed. R. M. Latanison and J. T. Fourie, Noordhoff, Reading, Mass., p. 801, 1977.

12. J. Lankford, D. L. Davidson, and T. S. Cook, "Fatigue Crack Tip Plasticity," Cyclic Stress-Strain and Plastic Deformation Aspects of Fatigue Crack Growth, ASTM STP 637, American Society for Testing and Materials, p. 36, 1977.

PUBLICATIONS (AFOSR Sponsorship) (Cont'd.)

13. J. Lankford and D. L. Davidson, "Fatigue Crack Tip Plastic Zone Sizes in Aluminum Alloys, International Journal of Fracture, April, 1978.

14. D. L. Davidson, "The Study of Fatigue Mechanisms with Electron Channeling," Fatigue Mechanisms, ASTM STP (in press).